

Semi-active control of a fluid viscous damper for vibration mitigation

F. Oliveira & P. Morais

Laboratório Nacional de Engenharia Civil (LNEC), Lisboa, Portugal

A. Suleman¹

Institute of Mechanical Engineering (IDMEC), Instituto Superior Técnico, Technical University of Lisbon (IST/UTL), Lisboa, Portugal

¹*Principal Investigator; also Professor, University of Victoria, Victoria, BC, Canada*



SUMMARY

In this paper the results of a study to evaluate the performance of several control algorithms for a hybrid system constituted by a base isolated structure plus a semi-active device are presented. A variable fluid damper at the base level is considered aiming to reduce earthquake induced vibrations. The performance of the algorithms is compared using a two degree of freedom dynamical model subjected to two different artificial accelerograms. The performance is evaluated by measuring the reduction in relative displacements and accelerations and comparisons are also made with passive and active systems. The results show that a semi-active sky-hook damper can be a viable option for structural vibration mitigation when the input has varying frequency content.

Keywords: Semi-active control, viscous damper, sky-hook damper, optimal control, vibration mitigation.

1. INTRODUCTION

Earthquakes have proven to be one of the most destructive natural disasters in the world. The traditional design methods for earthquake resistance of structures allow the occurrence of damage by using the inelastic deformation capacity of some elements. This kind of approach could be troublesome for structures that should be operational during and immediately after the occurrence of those events, such as: hospitals; energy power stations; communication centres; civil protection and fire station buildings. It is intended that structural relative displacements (inter-storey drifts) and accelerations are small in order to avoid damage and protect sensitive equipments from induced vibrations. The use of passive, semi-active (SA), active and hybrid control systems are typical ways of dealing with this problem; Soong and Spencer Jr. (2002). The semi-active control of seismically excited structures seems to be a promising proposal for civil engineering structures. The advantages of these systems compared with the others are: the capacity of adapting its characteristics in real time; the better overall performance when compared with passive devices; and lower power requirement, thus allowing for battery operation under proper conditions. A typical type of device that can be used for semi-active control is the fluid viscous variable damper. This type of devices consists typically of a hydraulic cylinder containing a piston which separates the two chambers that are connected by a hydraulic link. A control valve, like a solenoid valve or a servovalve is installed in the link to control the amount of fluid that flows from one chamber to the other. The control of the fluid through the valve can be performed in a continuous or in an on-off way; Symans and Constantinou (1999). In order to control the behaviour of those devices several control strategies have been proposed; Dyke (1996); Preumont (2002); Sadek and Mohraz (1998); Yoshida and Dyke (2004). One way to isolate the whole structure from ground motions and reduce both accelerations and inter-storey drifts is by using the base isolation concept; Kelly (1999). However, under near field actions increase in isolation displacement can lead to structural damage. An alternative solution is making use of hybrid systems (base isolation with active or semi-active devices); Shook *et al.* (2007).

In this paper the hybrid system is explored for controlling civil engineering structures subjected to earthquakes. Different control algorithms are presented and formulated for use with the SA device. Numerical simulations are made considering a two degree of freedom (2DOF) dynamic model employing an SA device with different control strategies and excited by two different input actions. Comparisons between the control algorithms and with passive and active systems are presented.

2. STRUCTURAL SYSTEM

The model considered in this study is a 2DOF system subjected to earthquake loads at the base (Fig. 1.1). It is intended to examine the earthquake response of base isolated structures having SA devices (variable damper) at the base level. A satisfactory approach considered in building's modelling is that: i) each floor has huge stiffness where the mass is concentrated; ii) the connections between floors are massless elements where the stiffness and damping is concentrated. In base isolated structures the superstructure is constructed over a base floor having a mass similar to the other floors which in turn is supported by bearings. For the purpose of this study the bearings are modelled as linear elastic and viscous damping elements. Additional damping is added at the base level by an additional device, which can be passive, active or semi-active. Fig. 1.1 shows a schematic view of the SA device considered in this study. The device consists of a hydraulic cylinder with a piston separating two chambers which are connected by a hydraulic link. One valve is used to control the flow from one chamber to the other. Although the mechanical behaviour of the device is non-linear (force proportional to the square of flow, or velocity) a linear relationship is assumed, which is similar to a linearization around the operating point. Using this approach one arrives to the linear viscous damping model (force proportional to velocity) where the damping coefficient is dependent on the valve opening. This approximation is useful in the sense that can easily provide information in terms of a damping coefficient. On the other hand, experimental tests have shown that this model is sufficient for describing the damper behaviour over the frequency range of interest for structural control applications; Symans and Constantinou (1999). The main purpose of the base isolated structure employing an SA device (variable damper) is: i) to reduce relative displacement between floors (inter-storey drifts), mainly due to structural physical constraints; ii) reduce absolute accelerations in order to improve human comfort and mitigate damage of delicate equipments installed in buildings; iii) reduce the relative displacement at the base level in order to reduce the costs associated with devices (bearings and dampers) and flexible utility connectors; Kelly (1999).

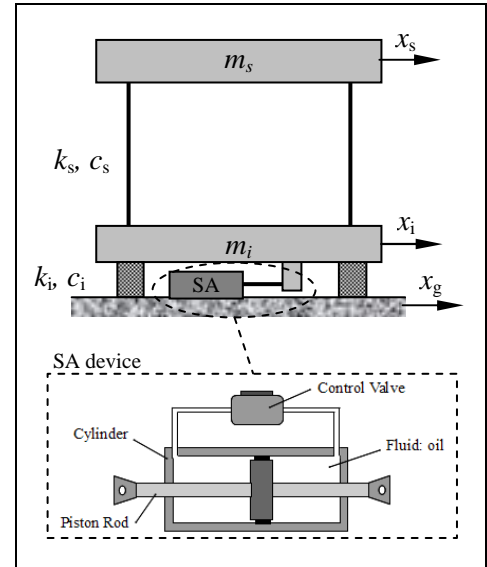


Figure 1.1. Structural System (2DOF) employing a semi-active (SA) variable damper.

The properties of the model considered in this study were evaluated taking into account the physical SDOF model with adjustable stiffness developed at LNEC for studying the seismic behaviour of structures employing different energy dissipation devices; Morais *et al.* (2010). For the superstructure a typical 8 floor composite steel building is considered. According to the RSA (1983) the fundamental frequency can be estimated as $f_1=16/n$, where 'n' is the number storeys, which in the present case leads to 2 Hz. The behaviour of the structure can be approximated by the behaviour of its first mode of vibration and thus simplified by a SDOF model. The first two expressions in Eqn. 2.1 are used to evaluate its natural frequency ' ω_s ' and damping ratio ' ζ_s ':

$$\omega_s = \sqrt{k_s/m_s}, \zeta_s = \frac{c_s}{2 \cdot m_s \cdot \omega_s}, \omega_i = \sqrt{\frac{k_i}{m_i + m_s}}, \zeta_i = \frac{c_i}{2 \cdot (m_i + m_s) \cdot \omega_i} \quad (2.1)$$

Taking into account the physical model mass $m_s=3750$ kg, the stiffness was adjusted (Eqn. 2.1) to $k_s=595$ kN/m in order to tune the fundamental frequency with the natural frequency of the SDOF physical system. With the damping ratio of $\zeta_s=6,4$ % the damping coefficient was evaluated (Eqn. 2.1): $c_s=6,05$ kN s/m. In order to reduce the fundamental frequency and increase the flexibility in the horizontal direction, low stiffness elements are introduced at the base level. This solution is called base isolation. An additional mode of vibration is added and the first one will have a shape with the superstructure vibrating over the bearings. The isolator natural frequency ' ω_i ' and damping ratio ' ζ_i '

are evaluated by the last two expressions in Eqn. 2.1. The characteristics considered for the isolation system are: mass $m_i=1000$ kg; stiffness $k_i=195$ kN/m; and a damping ratio of $\zeta_i=6,4$ %. The natural frequency and damping are then $f_i=1$ Hz and $c_i=3,90$ kN s/m (Eqn. 2.1). This base isolation concept is improved by modifying the damping at the base level with an SA device (hybrid system). Controlling the damping coefficient it is possible to change the dissipative force in order to improve the mechanical behaviour of the whole system (2DOF base isolation structure plus SA device). It is assumed that is possible to change the damping coefficient ' c_v ' between two values: a minimum value ' c_{min} ', corresponding to 5 % of additional damping (to sum with ζ_i); and a maximum one ' c_{max} ', corresponding to 77,2 % of additional damping (to sum with ζ_i); see sections 3.1 and 3.3.

The equations of motion of the system (Fig. 1.1) are given by:

$$\begin{aligned} m_i \cdot \ddot{x}_i + c_i \cdot (\dot{x}_i - \dot{x}_g) + c_s \cdot (\dot{x}_i - \dot{x}_s) + k_i \cdot (x_i - x_g) + k_s \cdot (x_i - x_s) &= f \\ m_s \cdot \ddot{x}_s + c_s \cdot (\dot{x}_s - \dot{x}_i) + k_s \cdot (x_s - x_i) &= 0 \end{aligned} \quad (2.2)$$

Eqn. (2.2) can be written in terms of relative quantities (accelerations, velocities and displacements) to the ground. The result can be expressed in a matricial form:

$$\begin{aligned} M_s \cdot \ddot{x}_{rg} + C_s \cdot \dot{x}_{rg} + K_s \cdot x_{rg} &= -M_s \cdot \mathbf{I}_{2,1} \cdot \ddot{x}_g + \mathbf{G} \cdot f \\ \begin{bmatrix} m_i & 0 \\ 0 & m_s \end{bmatrix} \begin{Bmatrix} \ddot{x}_{ig} \\ \ddot{x}_{sg} \end{Bmatrix} + \begin{bmatrix} c_i + c_s & -c_s \\ -c_s & c_s \end{bmatrix} \begin{Bmatrix} \dot{x}_{ig} \\ \dot{x}_{sg} \end{Bmatrix} + \begin{bmatrix} k_i + k_s & -k_s \\ -k_s & k_s \end{bmatrix} \begin{Bmatrix} x_{ig} \\ x_{sg} \end{Bmatrix} &= -\begin{bmatrix} m_i & 0 \\ 0 & m_s \end{bmatrix} \begin{Bmatrix} 1 \\ 1 \end{Bmatrix} \ddot{x}_g + \begin{Bmatrix} 1 \\ 0 \end{Bmatrix} f \end{aligned} \quad (2.3)$$

where: $\mathbf{x}_{rg}=[x_{ig} \ x_{sg}]^T=[x_i-x_g \ x_s-x_g]^T$ is the vector of relative displacements to the ground; the inter-storey drift is defined as ' $x_{si}=x_{sg}-x_{ig}$ '; ' \ddot{x}_g ' is the input acceleration at the base; ' M_s ', ' C_s ' and ' K_s ' are the mass, damping and stiffness matrices; ' $\mathbf{I}_{2,1}$ ' and ' \mathbf{G} ' are the unitary column vector and the column vector that defines the input forces location; and ' f ' is the input force in the system. If a semi-active fluid viscous device is used the force is given by:

$$f = f_{SA} = -c_v \cdot (\dot{x}_i - \dot{x}_g) = -c_v \cdot \dot{x}_{ig} \quad (2.4)$$

where ' c_v ' is the variable damping coefficient. By applying the Laplace transform to both expressions in Eqn. 2.2 the following transfer functions are obtained:

$$\begin{aligned} \begin{Bmatrix} A_i \\ A_s \end{Bmatrix} &= \begin{bmatrix} \frac{T_1}{1-T_2 \cdot T_3} & \frac{T_4}{1-T_2 \cdot T_3} s^2 \\ \frac{T_1 \cdot T_3}{1-T_2 \cdot T_3} & \frac{T_3 \cdot T_4}{1-T_2 \cdot T_3} s^2 \end{bmatrix} \begin{Bmatrix} A_g \\ F \end{Bmatrix}, \text{ with} \\ T_1 &= \frac{c_i \cdot s + k_i}{m_i \cdot s^2 + (c_i + c_s)s + k_i + k_s} \\ T_2 &= \frac{c_s \cdot s + k_s}{m_i \cdot s^2 + (c_i + c_s)s + k_i + k_s} \\ T_3 &= \frac{c_s \cdot s + k_s}{m_s \cdot s^2 + c_s \cdot s + k_s} \\ T_4 &= \frac{1}{m_i \cdot s^2 + (c_i + c_s)s + k_i + k_s} \end{aligned} \quad (2.5)$$

where: ' A_i ', ' A_s ', ' A_g ' and ' F ' are the Laplace transforms of ' \ddot{x}_i ', ' \ddot{x}_s ', ' \ddot{x}_g ' and ' f ' respectively; ' s ' is the complex variable. The terms ' T_i ' are individual transfer functions. Eqn. 2.5 can be used to obtain the system's absolute and relative displacements also. Another way to represent the system is in terms of state-space:

$$\begin{aligned} \dot{\mathbf{z}} &= \mathbf{A} \cdot \mathbf{z} + \mathbf{B} \cdot f + \mathbf{E} \cdot \ddot{x}_g, \text{ with } \mathbf{A} = \begin{bmatrix} 0_{2,2} & \mathbf{I}_2 \\ -\mathbf{M}_s^{-1} \cdot \mathbf{K}_s & -\mathbf{M}_s^{-1} \cdot \mathbf{C}_s \end{bmatrix}, \mathbf{B} = \begin{Bmatrix} 0_{2,1} \\ \mathbf{M}_s^{-1} \cdot \mathbf{G} \end{Bmatrix}, \mathbf{E} = \begin{Bmatrix} 0_{2,1} \\ -\mathbf{I}_{2,1} \end{Bmatrix} \\ \mathbf{y} &= \mathbf{C} \cdot \mathbf{z} + \mathbf{D} \cdot f \end{aligned} \quad (2.6)$$

where: $\mathbf{z} = \{x_{rg} \dot{x}_{rg}\}^T$ is the state vector; ' \mathbf{y} ' is the output vector, ' \mathbf{A} ' is the state matrix, ' \mathbf{B} ' and ' \mathbf{E} ' are input vectors; ' \mathbf{C} ' is the output matrix; ' \mathbf{D} ' is the feedthrough vector; ' $\mathbf{0}_{2,2}$ ' is a null matrix; ' $\mathbf{0}_{2,1}$ ' is a null vector, ' \mathbf{I}_2 ' is the identity matrix and ' $\mathbf{I}_{2,1}$ ' is the unitary vector. Matrices ' \mathbf{C} ' and ' \mathbf{D} ' are dependent on the selection of the output variables. Assuming that the output variables are the relative displacements between floors and the absolute accelerations, then:

$$C = \begin{bmatrix} 1 & 0 & 0 & 0 \\ -1 & 1 & 0 & 0 \\ -M_s^{-1} \cdot K_s & -M_s^{-1} \cdot C_s \end{bmatrix}, D = \begin{Bmatrix} \mathbf{0}_{2,1} \\ -M_s^{-1} \cdot \mathbf{G} \end{Bmatrix} \quad (2.7)$$

3. SEISMIC SAFETY USING PROTECTION SYSTEMS

3.1. Original and passive system

One way to easily analyse the response characteristics of the system is by looking to the locations of the system's poles in the Argand plane. This plot gives us information about the natural frequency and damping factors. The system's poles can be evaluated by finding the roots of the transfer functions denominator (Eqn. 2.5) or by finding the eigenvalues of matrix \mathbf{A} (Eqn. 2.6). The algebraic equation to solve is of fourth order:

$$(m_i \cdot m_s) p^4 + (c_i \cdot m_s + c_s \cdot m_i + c_s \cdot m_s) p^3 + (k_i \cdot m_s + k_s \cdot m_i + k_s \cdot m_s + c_i \cdot c_s) p^2 + (c_i \cdot k_s + c_s \cdot k_i) p + k_i \cdot k_s = 0 \quad (3.1)$$

where ' p ' are the solutions of the equation.

Assuming that the device attached to the system is a fluid viscous damper with a constant damping coefficient ' c_p ' then the system equations can be obtained by using the device force expression (Eqn. 2.4) with the passive device coefficient. Manipulating the equations it can be found that the result is equivalent to consider the system with a null input force ($f=0$) and a damping at the isolation system given by ' c_i+c_p '. The evolution of the system's poles as device's damping is increased is presented in Fig. 3.1. The correspondent natural frequencies and damping ratios can be extracted as shown in the same figure. Analysing the results it is found that the evolution of the poles as the damping ' c_p ' increases conducts to: i) larger damping ratios for mode 2 reaching the maximum damping when the poles achieve the real axis; ii) an increase in damping for the first mode until $\zeta_p=77,2\%$ ($\zeta_{isol}=\zeta_i+\zeta_p=83,6$) and thus $c_p=47$ kN s/m, which decreases thereafter. The original system's modal characteristics (for $\zeta_{isol}=\zeta_i=6,4\%$) are: $f_1=0,93$ Hz, $\zeta_1=5,3\%$; $f_2=4,82$ Hz, $\zeta_2=18,1\%$. With the passive damper at $\zeta_p=77,2\%$ are: $f_1=1,41$ Hz, $\zeta_1=67,7\%$; $f_2=3,15$ Hz, $\zeta_2=117\%$.

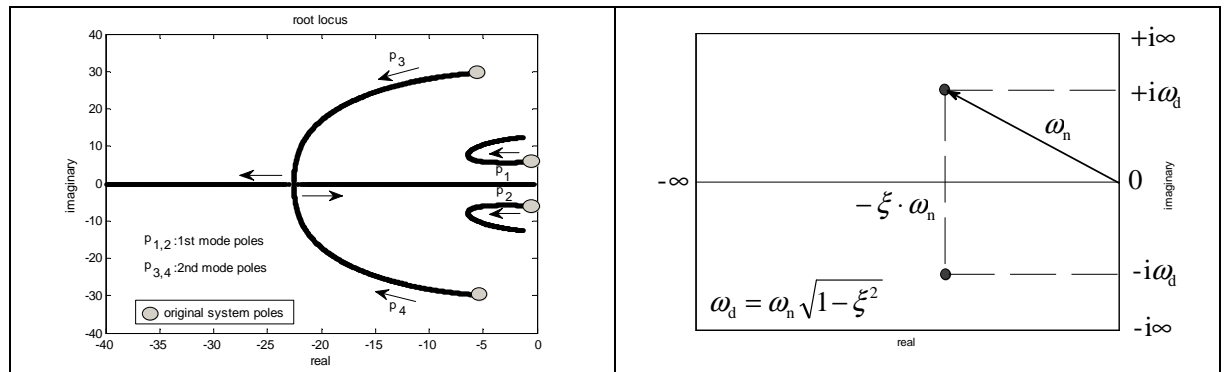


Figure 3.1. Left: Root locus for the system employing a passive device. Starts at original system's poles for an isolator damping $\zeta_{isol}=\zeta_i=6,4\%$. Right: Argand plane pole's representation: frequencies (damped and undamped) and damping factor.

Fig. 3.2 shows a comparison for three distinct cases in terms of magnitude curves of the transfer functions: original system; and with two passive cases. The position of the poles in the Argand plane is also shown. It is evident the influence of damping in the system's response. From this preliminary analysis it can be seen that a higher damping is needed for frequencies around the resonant frequency but smaller values are needed beyond the corner frequency in order to improve the isolation of higher frequencies namely on the relative displacement (inter-storey drift) and acceleration curves. To achieve these capabilities a variable damping device with an appropriate control law to change the damping coefficient in real time would be desired.

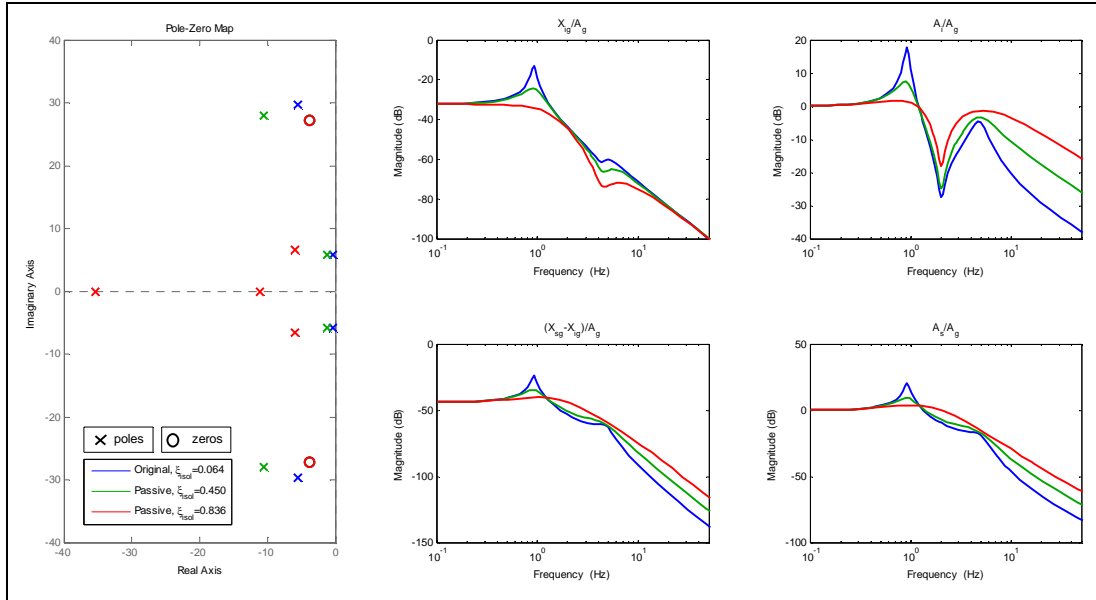


Figure 3.2. Left: Pole-zero map. Right: Bode diagram (magnitude) of the original 2DOF system $\zeta_{isol}=\zeta_i=6,4\%$ and with two passive cases ($\zeta_{isol}=45,0\%$ and $\zeta_{isol}=83,6\%$ with $\zeta_{isol}=\zeta_i+\zeta_p$), in terms of relative displacements between floors (X_{ig} and X_{si}) and absolute accelerations (A_i and A_s) relative to the input action (A_g).

3.2. Active Systems

On the other hand if an active device is attached to the system to improve its performance, a controller is needed to implement the control law obtained accordingly to a pre-established control strategy. In this work two different strategies are proposed to synthesize the controllers: acceleration feedback, also called 'sky-hook' (SH) damper, and the Linear Quadratic Regulator (LQR). Both of these controllers are also used in conjunction with the semi-active force feedback control. The generic control loop for the active system is presented in Fig. 3.3. For the purpose of this study it was assumed that the active device is an ideal sub-system, *i.e.* a transfer function with unitary gain in the frequency range of interest. So, ' f ' is equal to ' f_d '.

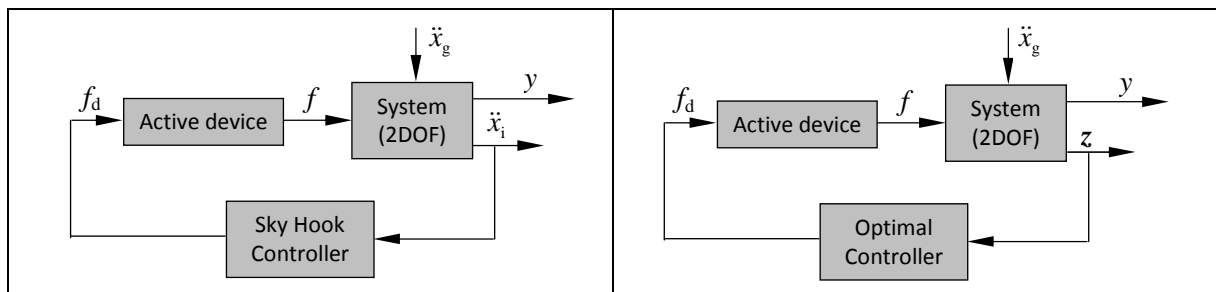


Figure 3.3. Control loop for the system employing an active device: with acceleration feedback (left); and optimal controller (right).

The sky-hook damper is described by Preumont (2002). The goal of this control strategy is to decrease the resonance peak without losing the isolation characteristics. This is made by using the acceleration

feedback path with an integral compensator so that the input control force is proportional to the absolute velocity. The control law is given by:

$$F = -g \cdot \frac{1}{s} \cdot s^2 X_i \quad (3.2)$$

where ‘ g ’ is the controller gain. Substituting Eqn. 3.2 in Eqn. 2.5 the transfer functions of the closed loop system are obtained:

$$\frac{A_i}{A_g} = \frac{T_1}{1 - T_2 \cdot T_3 + g \cdot s \cdot T_4}, \quad \frac{A_s}{A_g} = \frac{T_1 \cdot T_3}{1 - T_2 \cdot T_3 + g \cdot s \cdot T_4} \quad (3.3)$$

The system’s poles can be evaluated by finding the roots of the transfer functions denominator. The algebraic equation to solve is identical to Eqn. 3.1 but with ‘ c_i+g ’ instead of ‘ c_i ’. The root locus is similar to the one found in Fig. 3.1. The gain value that dampens more the system poles is $g=47$ kN s/m. This value is identical to the coefficient found for the passive system but the advantage here is that the gain doesn’t affect the system zeros (numerator of the transfer functions) and thus maintains the isolation characteristics at higher frequencies. The poles are then in the same location of the passive system’s poles. However, the relative displacements of the base are increased in the lower frequencies range (see Fig. 3.4).

As mentioned previously an optimal controller was also synthesised for the purpose of this study. Assuming that the input seismic action ‘ \ddot{x}_g ’ is a white noise excitation with zero mean and intensity (variance) ‘ I_{xg} ’, the LQR problem was formulated. Since the system is controllable, the goal is to find the control action ‘ f ’ for the system described by Eqn. 2.6 that minimizes a performance index that weights a generic output ‘ y_g ’ and the input control force ‘ f ’ (Dyke, 1996):

$$J = \lim_{\tau \rightarrow \infty} \frac{1}{\tau} E \left[\int_0^{\tau} y_g^T \cdot Q_g \cdot y_g + r \cdot f^2 d\tau \right] \quad (3.4)$$

where ‘ Q_g ’ is a diagonal matrix that weights the correspondent output, and ‘ r ’ weights the control action. The solution is given by the following constant gain linear state feedback:

$$f = -K_y \cdot \mathbf{z}, \text{ with } K_y = B^T P / r \quad (3.5)$$

where ‘ K_y ’ is the constant and ‘ P ’ is the solution of the algebraic Riccati equation; Dyke (1996). The closed loop system is then given by:

$$\begin{aligned} \dot{\mathbf{z}} &= (A - B \cdot K_y) \cdot \mathbf{z} + G \cdot \ddot{x}_g \\ \mathbf{y}_g &= (C_g - D_g \cdot K_y) \cdot \mathbf{z} \end{aligned} \quad (3.6)$$

The LQR problem assumes that all states (relative displacement and relative velocity) are available at all time instants. However, in most practical situations the measurement of the states is not always feasible, can be complex or even very expensive. In such cases, if the system is observable the states can be estimated from a model of the system along with the output and input measurements – observer design; Preumont (2002). This analysis is focused on the system’s performance hence the observer design was not taken into account. With the presented formulation a preliminary analysis was made in order to identify the weights that are more beneficial for the system’s response. It was found that the best way to reduce the resonance peaks without compromising the higher frequency decay is mainly by weighing the inter-storey drift ‘ x_{si} ’ or the acceleration of the second floor ‘ \ddot{x}_s ’ having the control force weight ‘ r ’ fixed. If each of those weights are fixed then the increase of the control force weight ‘ r ’ conducts to the inverse evolution verified when weighting the responses. The values chosen to synthesize the optimal controller were: base mass acceleration weight $q_{ai}=0,05$; structure’s mass

acceleration weight $q_{as}=0,3$; and force weight $r=10^{-10}$. As with the sky-hook damper the active optimal controlled system amplifies the relative displacements in the lower frequency range although good performances are found on to other variables (Fig. 3.4).

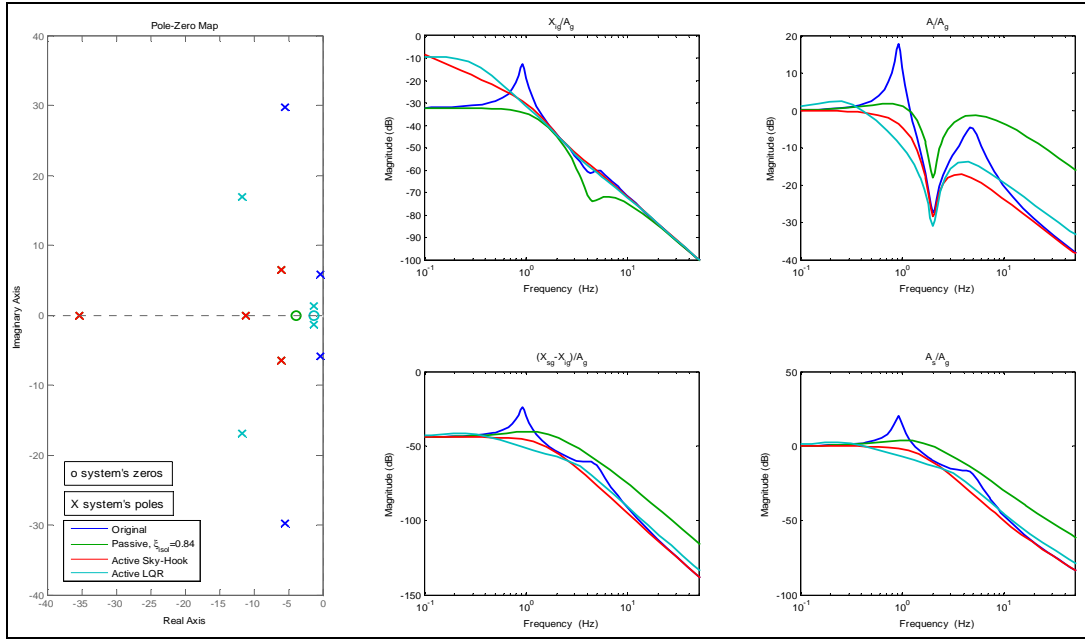


Figure 3.4. Left: Pole-zero map. Right: Bode diagram (magnitude) of the original 2DOF system $\zeta_{isol}=\zeta_i=6,4\%$ and employing a passive device ($\zeta_{isol}=83,6\%$ with $\zeta_{isol}=\zeta_i+\zeta_p$), an active sky-hook damper and an active LQR controller. Results in terms of relative displacements between floors (X_{ig} and X_{si}) and absolute accelerations (A_i and A_s) relative to the input action (A_g).

3.3. Semi-Active Systems

This section describes the semi-active control strategies used in this study. It is assumed that the semi-active device has an ideal transfer function and the damping coefficient ' c_v ' can be changed between $c_{min}=3$ kN s/m, corresponding to $\zeta_v=5\%$ of additional damping (to sum with ζ_i) and $c_{max}=47$ kN s/m, corresponding to $\zeta_v=77,2\%$ of additional damping. Two strategies were adopted: Bang-bang control; and force feedback control. The first strategy only needs the system's responses to define the best damping coefficient. The control loop is represented in Fig. 3.5.

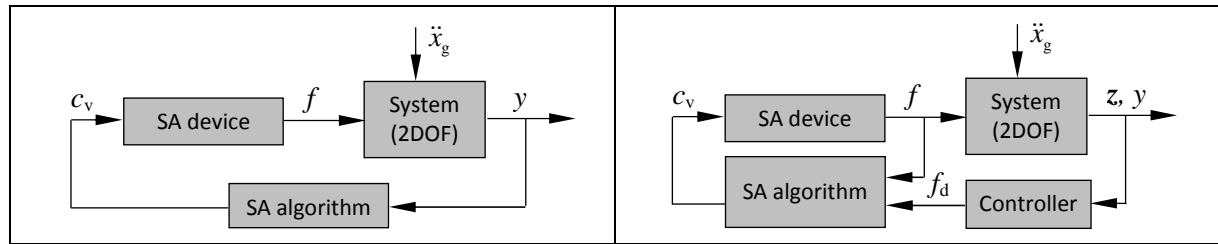


Figure 3.5. Bang-bang semi-active control loop (left); force feedback semi-active control loop (right).

This control strategy is based on the Lyapunov stability theory. The Lyapunov function chosen represents the total vibratory energy in the structure (kinetic plus potential energy), and thus the algorithm that results is called **Decentralized Bang-Bang control (DBB)**; Jansen and Dyke (2000). The control law that makes the Lyapunov function as large and negative as possible is given by:

$$c_v = c_{max} \mathbf{H}\left[-(\dot{x}_{rg} + \mathbf{I}_{2,1} \cdot \dot{x}_g)^T \cdot \mathbf{G} \cdot f\right] = c_{max} \mathbf{H}\left[\dot{x}_i \cdot \dot{x}_{ig}\right], \text{ with } c_{min} \leq c_v \leq c_{max} \quad (3.7)$$

where $\mathbf{H}[\cdot]$ is the Heaviside step function.

The second strategy needs the path from the controller, designed for the active devices, which determines the desired control force ' f_d '. This one in conjunction with the path of the force developed by the device ' f ' are feedthrough to the SA algorithm which determines the best damping coefficient to input in the SA device. The control loop is also shown in Fig. 3.5. With this control strategy the damping coefficient will be chosen so that the device's force follows the desired one evaluated by the controller. However, according to the nature of the device, the algorithms assume that is only possible to oppose force (energy dissipation), and thus the damping coefficient will be changed only when the desired force and damper force have the same sign. The controllers used in the loop are the ones synthesised in the previous subsection. In what concerns the algorithms two types can be found: on-off and continuous control laws.

The **variable damping** (VD) control law consists in changing the damper coefficient according to the desired force using the device's mathematical model and taking into account the device's physical limits. This algorithm was used by Sadek and Mohraz (1998) in their studies:

$$c_v = -\frac{f_d}{\dot{x}_{ig}}, \text{ with } c_{\min} \leq c_v \leq c_{\max} \quad (3.8)$$

Another semi-active control strategy consists in defining a clipping algorithm that tries to make the semi-active device to replicate the desired force resulting from the controller. The **clipped continuous control** (CCC) consists in defining a proportional gain ' g_p ' applied to the difference between absolute forces. This gain should be selected according to the control objectives; Preumont (2002). The semi-active control law is given by:

$$c_v = g_p (|f_d| - |f|) \cdot \mathbf{H}[(f_d - f) \cdot f], \text{ with } c_{\min} \leq c_v \leq c_{\max} \quad (3.9)$$

If the proportional gain is very large the control algorithm becomes an on-off algorithm which is described as the **clipped on-off** (COO) algorithm. When used in conjunction with an optimal controller it is called clipped optimal control algorithm; Dyke (1996). The control law is simplified to:

$$c_v = c_{\max} \cdot \mathbf{H}[(f_d - f) \cdot f], \text{ with } c_{\min} \leq c_v \leq c_{\max} \quad (3.10)$$

Yoshida and Dyke (2004) refer that in certain situations the COO algorithm lead to high local accelerations. These authors proposed a **modified clipped on-off algorithm** (MCOO) consisting in continuously changing the control variable (damping coefficient in this case) by applying a proportional gain ' c_{\max}/f_{\max} ' on the desired force. This semi-active control law is given by:

$$c_v = \begin{cases} \frac{c_{\max}}{f_{\max}} \cdot |f_d| \cdot \mathbf{H}[(f_d - f) \cdot f], & \text{for } |f_d| \leq f_{\max} \\ c_{\max}, & \text{for } f_d > f_{\max} \end{cases}, \text{ with } c_{\min} \leq c_v \leq c_{\max} \quad (3.11)$$

4. NUMERICAL SIMULATIONS

The semi-active fluid damper capabilities were evaluated and compared with the passive and the active devices in the 2DOF system described. The different control algorithms described were used. For this purpose it was considered that all states and variables are available for measurement. In terms of seismic actions, it is well known that earthquakes are characterized as non-stationary stochastic processes whose amplitude and frequency content change during its occurrence. On the other hand, the seismic action is also dependent on several factors like the generation and propagation effects and the local effects, which determine its amplitude and frequency content; Carvalho (2007). In the simulation studies two different input actions were considered to analyse the system's performance. The input actions are artificial accelerograms generated using the extreme response spectrums provided in the Eurocode 8 for Portugal, for the two types of seismic actions, in zone 1. The soil type D was considered and the importance factors of the structures were set to 1 (importance class II). The two

input actions generated for the simulations are: 1) a type 1 seismic action: EC8DNA11DIIacel; 2) type 2 seismic action: EC8DNA21DIIacel. The accelerograms and the spectrums are presented in Fig. 4.1. As shown in the figure, type 1 input action has a longer duration and is richer in the lower frequencies.

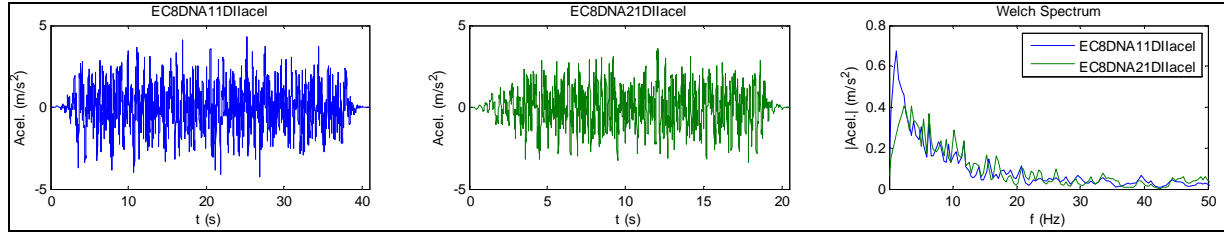


Figure 4.1. Input actions considered in the numerical simulations. Left: type 1 seismic action, EC8DNA11DIIacel. Middle: type 2 seismic action, EC8DNA21DIIacel. Right: Both actions' spectrums.

Simulations were made using the MATLAB/Simulink environment. The system's performance was evaluated in terms of peak values and RMS values of the whole output time signal considering those two inputs. The ratios showing the percent reduction compared to the original structure's values are also presented in brackets. Table 4.1 shows the results of the evaluation criterion indices for the various system's configurations: i) open-loop system (original, no control); ii) Passive (structure with a passive device at maximum damping); iii) active system (SH and LQR); iii) semi-active systems (DBB, and the combinations of controllers 'SH' and 'LQR' with the algorithms 'VD', 'CCC', 'COO' and 'MCOO'). The algorithms 'CCC' and 'MCOO' considered the gain which attained the best response, as indicated next to the algorithm designation in Table 4.1 (' g_p ' and ' c_{vmax}/f_{max} ' respectively).

Table 4.1. System's performance results in terms of evaluation criterion indices.

Input Action	EC8DNA11DIIacel (type 1 action)								EC8DNA11DIIacel (type 2 action)							
	rms x_{ig}	peak x_{ig}	rms x_{si}	peak x_{si}	rms \ddot{x}_i	peak \ddot{x}_i	rms \ddot{x}_s	peak \ddot{x}_s	rms x_{ig}	peak x_{ig}	rms x_{si}	peak x_{si}	rms \ddot{x}_i	peak \ddot{x}_i	rms \ddot{x}_s	peak \ddot{x}_s
Evaluat. Indices	(mm)	(mm)	(mm)	(mm)	(m/s ²)	(m/s ²)	(m/s ²)	(m/s ²)	(mm)	(mm)	(mm)	(mm)	(m/s ²)	(m/s ²)	(m/s ²)	(m/s ²)
absolute values	& %	& %	& %	& %	& %	& %	& %	& %	& %	& %	& %	& %	& %	& %	& %	& %
(percent reduction)																
Original System	57,3	164,0	15,6	44,8	1,96	5,52	2,48	7,13	22,2	58,9	6,1	16,2	0,80	2,34	0,97	2,58
Passive	13,6 (76)	39,2 (76)	7,4 (52)	22,6 (50)	0,98 (50)	3,28 (41)	1,18 (52)	3,60 (49)	5,6 (75)	17,5 (70)	3,8 (37)	13,7 (15)	0,74 (7)	2,44 (-4)	0,61 (37)	2,20 (15)
SH	31,4 (45)	95,2 (42)	3,8 (76)	10,9 (76)	0,46 (76)	1,46 (74)	0,60 (76)	1,73 (76)	13,0 (41)	31,2 (47)	1,6 (73)	5,0 (69)	0,20 (75)	0,63 (73)	0,26 (73)	0,79 (69)
LQR	43,1 (25)	130,1 (21)	2,6 (83)	7,3 (84)	0,36 (82)	1,08 (81)	0,41 (83)	1,17 (84)	18,0 (19)	39,9 (32)	1,2 (81)	4,2 (74)	0,20 (75)	0,64 (73)	0,19 (81)	0,68 (74)
DBB	17,6 (69)	53,3 (68)	6,7 (57)	24,5 (45)	1,35 (31)	13,28 (-140)	1,07 (57)	3,90 (45)	8,0 (64)	23,8 (60)	3,1 (49)	12,8 (21)	0,71 (11)	8,17 (-249)	0,49 (49)	2,05 (21)
SH VD	20,6 (64)	60,9 (63)	6,6 (58)	22,4 (50)	0,96 (51)	3,96 (28)	1,06 (58)	3,57 (50)	8,8 (60)	25,5 (57)	2,9 (53)	8,1 (50)	0,56 (30)	2,31 (1)	0,46 (53)	1,30 (50)
SH COO	20,4 (64)	59,1 (64)	6,6 (58)	19,8 (56)	2,12 (-8)	16,03 (-190)	1,05 (58)	3,18 (55)	8,7 (61)	25,0 (58)	2,9 (53)	10,9 (33)	1,01 (-27)	6,76 (-189)	0,46 (52)	1,75 (32)
SH CCC 2,5	26,3 (54)	76,1 (54)	7,5 (52)	21,4 (52)	0,98 (50)	3,46 (37)	1,20 (52)	3,41 (52)	12,0 (46)	39,8 (32)	3,5 (43)	10,5 (35)	0,52 (34)	2,10 (10)	0,55 (43)	1,67 (35)
SH MCOO 2,236	23,8 (58)	67,1 (59)	7,2 (54)	20,6 (54)	0,95 (52)	3,91 (29)	1,14 (54)	3,29 (54)	11,6 (48)	36,7 (38)	3,4 (44)	10,6 (35)	0,52 (34)	2,23 (5)	0,54 (44)	1,69 (35)
LQR VD	31,0 (46)	96,3 (41)	7,7 (51)	26,7 (40)	1,07 (45)	4,57 (17)	1,22 (51)	4,26 (40)	12,1 (45)	39,3 (33)	3,1 (49)	11,3 (30)	0,53 (33)	1,90 (19)	0,49 (49)	1,80 (30)
LQR COO	24,5 (57)	70,4 (57)	7,1 (54)	22,5 (50)	2,76 (-41)	13,77 (-149)	1,14 (54)	3,60 (49)	10,0 (55)	31,7 (46)	3,1 (50)	12,2 (25)	1,23 (-54)	7,24 (-209)	0,49 (50)	1,95 (24)
LQR CCC 2	41,7 (27)	115,2 (30)	11,1 (29)	32,1 (28)	1,44 (27)	4,29 (22)	1,77 (29)	5,10 (28)	16,4 (26)	52,1 (12)	4,6 (25)	13,9 (14)	0,64 (20)	2,31 (1)	0,73 (25)	2,22 (14)
LQR MCOO 1,423	40,4 (30)	113,6 (31)	10,8 (31)	31,8 (29)	1,40 (29)	4,27 (23)	1,72 (31)	5,06 (29)	16,5 (25)	52,2 (11)	4,6 (24)	14,0 (14)	0,64 (19)	2,31 (1)	0,73 (24)	2,22 (14)

The results show that in general all the solutions can reduce both relative displacements and accelerations although the SA devices working with on-off algorithms (DBB and COO) lead to higher accelerations at the base mass. The passive device is the best at reducing the relative displacement of the base mass but at the expense of penalising the other variables, especially when the input is a type 2 action. On the other hand, with the active hybrid system (base isolation plus active devices) the base relative displacements are slightly superior to the ones for the passive device, but in terms of the remaining variables indices the results are the best ones. It is found that the SH is better than LQR in

terms of base relative displacements but at the expense of loosing some performance on the remaining variables indices. When using a semi-active hybrid system (base isolation plus semi-active device), the best solution is the SH controller with VD algorithm. This configuration can reduce both accelerations and inter-storey drifts, always better than the passive case, but at the coast of penalising a little bit the relative displacement of the base mass. However this was the cost assumed by reducing the accelerations and inter-storey drifts. The results show also that this configuration is manly effective with type 2 action as input, having a similar performance to the passive case when a type 1 action is considered. The LQR VD shows also better performance than the passive case but only when a type 2 action is considered. Another aspect to mention (not shown) is that COO algorithms, CCC with higher gains and MCOO with lower gains have always some chattering in the acceleration responses. Even choosing an optimized gain the performance of these algorithms is inferior to the SH VD.

5. CONCLUSIONS

An alternative solution to the usage of passive or active systems to reduce earthquake induced vibrations has been presented. The main idea consists in changing the damping of a passive device in real time. In order to reduce both inter-storey drifts and accelerations this concept was used in conjunction with a base isolation system. Several control strategies were formulated for use with this type of devices. Numerical simulations of a 2DOF dynamic model were performed with the SA control strategies and also with the passive and active devices. The results showed that SA hybrid systems can reduce both inter-storey drift and accelerations for the two input actions considered. The SH VD (sky-hook with variable damping) was found to be the best SA control strategy. The LQR counterpart showed better performance than the passive only when a type 2 action is considered. Although active devices present better performance than SA ones, they are always more expensive and need a huge power supply to operate it. In summary, the only semi-active system that performs better than the passive considering the two inputs is the SH VD. So, further studies should be conducted considering other accelerograms for other zones and other soil types.

REFERENCES

- Carvalho, A. (2007). Modelação da Acção Sísmica em Portugal. PhD Thesis. Instituto Superior Técnico, Universidade Técnica de Lisboa. (in Portuguese).
- Dyke, S.J. (1996). Acceleration Feedback Control Strategies for Active and Semi-Active Control Systems: Modeling, Algorithm Development and Experimental Verification. PhD Thesis. University of Notre Dame. Indiana.
- Jansen, L.M. and Dyke, S.J. (2000). Semi-Active Control Strategies for MR Dampers: A Comparative Study. *Journal of Engineering Mechanics* **126(8)**: 795–803.
- Kelly, J.M. (1999). The Role of Damping in Seismic Isolation. *Earthquake Engineering and Structural Dynamics* **28**: 3-20.
- Morais, P.G. Oliveira, F.V. Falcão, M.J. Campos Costa, A. (2010). Sistema Mecânico para Simulação Física do Comportamento Dinâmico de Estruturas. *Acta do 8º Congresso Nacional de Mecânica Experimental*, Guimarães, 21-23 de Abril. (in Portuguese).
- Preumont, A. (2002). *Vibration Control of Active Structures – An Introduction* (2nd edition). Kluwer Academic Publishers.
- R.S.A. (1983). Regulamento de Segurança e Acções para Estruturas de Edifícios e Pontes. Decreto- Lei nº **235/83**. *Imprensa Nacional – Casa da Moeda, E. P.*, Lisbon, Portugal. (in Portuguese).
- Sadek, F. and Mohraz, B. (1998). Semiactive control algorithms for structures with variable dampers. *Journal of Engineering Mechanics* **124(9)**.
- Shook, D. Lin, P. Lin, T. and Roschke, P.N. (2007). A comparative study in the semi-active control of isolated structures. *Smart Materials and Structures* **16**:1433–1446.
- Soong, T.T. and Spencer, Jr. B.F. (2002). Supplemental energy dissipation: state-of-the-art and state-of-the practice. *Engineering Structures* **24**:243–259.
- Symans, M.D., Constantinou, M.C. (1999). Semi-active control systems for seismic protection of structures: a stateof-the-art review. *Engineering Structures* **21**: 469–487.
- Yoshida, O. and Dyke, S.J. (2004). Seismic Control of a Nonlinear Benchmark Building Using Smart Dampers. *Journal of Engineering Mechanics* **130(4)**.